

Broadband Dichromatic Variational Measurement

Sergey P. Vyatchanin,^{1,2} Albert I. Nazmiev,¹ and Andrey B. Matsko³

¹*Faculty of Physics, M.V. Lomonosov Moscow State University, Leninskie Gory, Moscow 119991, Russia*

²*Quantum Technology Centre, M.V. Lomonosov Moscow State University, Leninskie Gory, Moscow 119991, Russia*

³*Jet Propulsion Laboratory, California Institute of Technology,
4800 Oak Grove Drive, Pasadena, California 91109-8099, USA*

(Dated: October 25, 2021)

Standard Quantum Limit (SQL) of a classical mechanical force detection results from quantum back action impinging by the meter on a probe mechanical transducer perturbed by the force of interest. In this paper we introduce a technique of continuous **broadband** back action avoiding measurements for the case of a resonant signal force acting on a linear mechanical oscillator supporting one of mirrors of an optical Michelson-Sagnac Interferometer (MSI). The interferometer with the movable mirror is an opto-mechanical transducer able to support polychromatic probe field. The method involves a dichromatic optical probe resonant with the MSI modes and having frequency separation equal to the mechanical frequency. We show that analyzing each of the harmonics of the probe reflected from the mechanical system separately and postprocessing the measurement results allows excluding the back action in a broad frequency band and measuring the force with sensitivity better than SQL.

I. INTRODUCTION

Optical transducers are frequently used for observation of mechanical motion. They allow measuring displacement, speed, acceleration, and rotation of mechanical systems. Mechanical motion can change frequency, amplitude and phase of the probe light, that is processed to obtain information about the motion. The measurement sensitivity can be extremely high. For instance, a relative mechanical displacement orders of magnitude smaller than a proton size can be detected. This feature is utilized in gravitational wave detectors [1–6], in magnetometers [7, 8], and in torque sensors [9–11].

The fundamental sensitivity limitations of the measurement always were of interest. One of the limits results from the fundamental thermodynamic fluctuations of the probe mechanical system. The absolute position detection is restricted due to the Nyquist noise. However, this obstacle can be removed if one intends to measure a variation of the position, not its absolute value. The thermal noise does not limit sensitivity of the measurement that occurs much faster than the system ringdown time.

Another limitation comes from the quantum noise of the meter. On one hand, the accuracy of the measurements of the observables of the meter is restricted because of their fundamental quantum fluctuations, represented by the shot noise for the optical probe wave. On the other hand, the sensitivity is impacted by the perturbation of the state of the probe mass due to the mechanical action of the meter on the mass. This effect is called “quantum back action”. In the case of optical meter the mechanical perturbation results from the pressure of light. Interplay between these two phenomena results in so called standard quantum limit (SQL) [12, 13] of the measurement sensitivity.

The value of the SQL depends on the measurement system as well as the measurement strategy and measure-

ment observable. In the case of the detection of a classical force acting on a mechanical probe mass, the SQL can be avoided in a configuration supporting opto-mechanical velocity measurement [14, 15]. The limit also can be surpassed using opto-mechanical rigidity [16, 17]. Preparation of the probe light in a nonclassical state [18–24] as well as detection of a variation of a strongly perturbed optical quadrature [25–27] curbs the quantum back action and lifts SQL. The back action and SQL can be avoided with coherent quantum noise cancellation [28–30] as well as compensation using an auxiliary medium with negative nonlinearity [31].

Optimization of the detection scheme by utilizing a few optical frequency harmonics as a probe allows beating the SQL of a force detection. The technique was introduced forty years ago [32, 33] and then expanded to various measurement configurations [34–38]. Additionally, usage of a dichromatic optical probe in a resonant optical transducer may lead to observation of such phenomena as negative radiation pressure [39, 40], optical quadrature-dependent quantum back action [25, 27, 41, 42] as well as mechanical velocity-dependent interaction [14, 15]. All these phenomena are useful for back action suppression.

Noncommutativity between the probe noise and the quantum back action noise is the reason for SQL. In a simple displacement sensor the probe noise is represented by the phase noise of light and the back action noise depends on the amplitude noise of light. The signal is contained in the phase of the probe. The relative phase noise decreases with optical power. The relative back action noise increases with the power. The signal to noise ratio optimizes at a specific power value. The optimal measurement sensitivity corresponds to SQL. Because phase and amplitude quantum fluctuations of the same wave do not commute, it is not possible to measure the amplitude noise and subtract it from the measurement result.

In this paper we suggest a measurement procedure that allows post-processing of the measurement result

and subtracting the quantum back action contribution. The measurement takes advantage of usage of a dichromatic optical probe in a resonant displacement transducer. We show that the signal results in modification of the power distribution between the spectral components of the probe, while the back action is proportional to the total power of the probe harmonics. Fundamentally, the power difference and total power can be measured independently. As the result, the quantum back action can be removed from the measurement result by post-processing of the measurement results.

In the measurement procedure the probe mass is strongly perturbed. In this way the technique has similar spirit with the variational approach leading to accurate measurement of a variation of a quantum systems in spite of the strong perturbation of the system parameters. Unlike standard variational measurement, the described here technique is broadband. The back action can be removed at all spectral frequencies.

The proposed here technique is especially efficient when the signal force is resonant with the mechanical probe mass suspension. In this regime the external force modifies the power redistribution between the probe spectral components most efficiently. The variational measurement technique based on a monochromatic probe light does not perform well in this case.

The paper is organized as follows. The physical model of the measurement system is introduced in Section II. The mean amplitudes of the system parameters, the quantum fluctuations and associated noise components are studied in Section III. The optimal sensitivity of the measurement is also found in this Section. The impact of the parasitic sidebands is analyzed in Section IV. Section V concludes the paper.

II. PHYSICAL MODEL

Let us consider an opto-mechanical system consisting of two externally pumped optical modes coupled with each other and with a mechanical oscillator (Fig. 1). The difference between the optical mode frequencies is equal to the frequency of the mechanical oscillator. In what follows we show feasibility of the broadband detection of a small signal force acting on the mechanical oscillator while keeping sensitivity of the measurement better than the SQL.

The opto-mechanical system can be realized in a ring cavity with coupled clockwise and counterclockwise modes. The uncoupled modes are frequency degenerate. Let us assume that their frequency is equal to ω_0 . Introducing a membrane inside the cavity (see Fig. 1) removes degeneracy and frequencies of the modes split (so called coherent coupling [43])

$$\omega_- = \omega_0 - |\kappa|, \quad \omega_+ = \omega_0 + |\kappa|, \quad (2.1)$$

where splitting factor κ depends on transparency of the membrane as well as on its position. Parameter κ is a

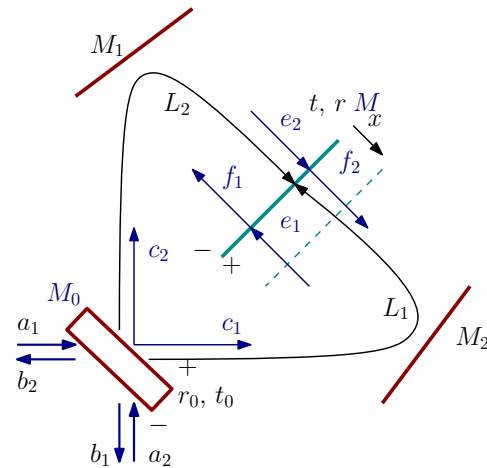


Figure 1: High-finesse ring cavity with input mirror M_0 with transmission t_0 and reflectivity r_0 ($t_0 \ll r_0$) and dielectric mirror M (membrane) inside with transmission t and reflectivity r ($r \ll t$).

complex value. Specific feature of coherent coupling is such that the absolute value of $|\kappa|$ depends on optical parameters of the membrane and phase of κ depends on the membrane position [43].

Another example of a scheme enabling the back action evading measurement is the Michelson-Sagnac interferometer (MSI) shown in Fig. 2. The system also has two degenerate modes. If the position of a perfectly reflecting mirror M is fixed, one MSI mode, characterized with frequency ω_+ , is given by a light wave which travels between M_1 and BS. The light is split on the BS and after reflection from mirror M returns exactly to M_1 . It does not propagate to M_2 . The other mode, characterized with frequency ω_- , is represented by a wave which travels from M_2 to BS and after reflection from M returns to M_2 and does not propagate to M_1 . The frequencies of the modes, ω_{\pm} , are controlled by variation of path distances ℓ_1, ℓ_2 . Variation of the position of mirror M provides coupling between the modes. Mirror M is a test mass of the mechanical oscillator with mass m and eigenfrequency ω_m .

A. Main assumptions

Let us consider scheme shown in Fig. 2. We assume that the relaxation rates of the eigen modes are identical and characterized with the full width at the half maximum (FWHM) equal to 2γ . The mechanical relaxation rate is small if compared with the optical one: $\gamma_m \ll \gamma$. We also assume that the conditions of the resolved side band interaction and frequency synchronisation are valid:

$$\gamma_m \ll \gamma \ll \omega_m, \quad \omega_+ - \omega_- = \omega_m \quad (2.2)$$

The resonance curves shown in the right panel of Fig. 2 illustrate the conditions accepted above.

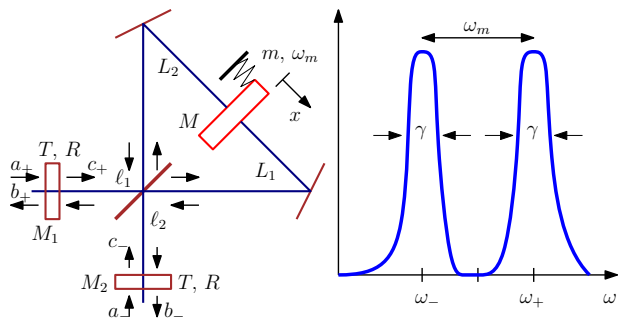


Figure 2: Schematic of the Michelson-Sagnac interferometer in which mirror M is completely reflecting. The mirror is a test mass m of the mechanical oscillator with frequency ω_m . Two eigenmodes with frequencies ω_- , ω_+ are coupled with the mechanical oscillator. Relaxation rate γ is the same for the both modes, $\gamma \ll \omega_m$. Modes ω_{\pm} are resonantly pumped.

For the sake of simplicity we also assume that following conditions are valid

$$L_1 \simeq L_2, \quad L_1, L_2 \gg \ell_1, \ell_2. \quad (2.3)$$

B. Hamiltonian

The generalized Hamiltonian describing the system can be presented in form

$$H = H_0 + H_{\text{int}} + H_T + H_{\gamma} + H_{T,m} + H_{\gamma_m}, \quad (2.4a)$$

$$H_0 = \hbar\omega_+ c_+^{\dagger} c_+ + \hbar\omega_- c_-^{\dagger} c_- + \hbar\omega_m d^{\dagger} d, \quad (2.4b)$$

$$H_{\text{int}} = \frac{\hbar}{i} \left(\eta c_+^{\dagger} c_- d - \eta^* c_+ c_-^{\dagger} d^{\dagger} \right). \quad (2.4c)$$

H_{int} is the Hamiltonian of the interaction between modes, d , d^{\dagger} are annihilation and creation operators of the mechanical oscillator, c_{\pm} , c_{\pm}^{\dagger} are annihilation and creation operators of the corresponding optical modes. The operator of coordinate x of the mechanical oscillator can be presented in form

$$x = x_0 (d + d^{\dagger}), \quad x_0 = \sqrt{\frac{\hbar}{2m\omega_m}}. \quad (2.5)$$

The coupling constant η can be written as

$$|\eta| \simeq \frac{x_0}{L} \omega_0, \quad L \simeq L_1, L_2, \quad \omega_0 \simeq \omega_{\pm} \quad (2.6)$$

H_T is the Hamiltonian describing the environment (thermal bath) and H_{γ} is the Hamiltonian of the coupling between the environment and the optical modes resulting in decay rate γ . Similarly, $H_{T,m}$ is the Hamiltonian of the environment and H_{γ_m} is the Hamiltonian describing coupling between the environment and the mechanical oscillator resulting in decay rate γ_m . See Appendix A for details.

It is convenient to separate the expectation values of the wave amplitudes as well as their fluctuation parts and assume that the fluctuations are small:

$$\mathcal{A}_{\pm} = (A_{\pm} + \hat{a}_{\pm}) e^{-i\omega_{\pm} t}, \quad (2.7)$$

$$\mathcal{B}_{\pm} = (B_{\pm} + \hat{b}_{\pm}) e^{-i\omega_{\pm} t}. \quad (2.8)$$

A_{\pm} and B_{\pm} stand for the expectation values of the amplitudes of the corresponding optical waves and a_{\pm} and b_{\pm} represent the fluctuations, $|A_{\pm}|^2 \gg \langle a_{\pm}^{\dagger} a_{\pm} \rangle$ and $|B_{\pm}|^2 \gg \langle b_{\pm}^{\dagger} b_{\pm} \rangle$, where $\langle \dots \rangle$ stands for ensemble averaging.

The normalization of the amplitudes is selected so that $\hbar\omega_{\pm}|A_{\pm}|^2$ describes the optical power [27]. We also consider only spectral components around carrier frequencies ω_{\pm} and drop the harmonics centered at frequencies $(\omega_+ + \omega_m)$ and $(\omega_- - \omega_m)$ far from the corresponding resonances.

The Hamiltonian of the system allows us to write the equations of motion for the intracavity fields. The complete derivation of these equations is presented in Appendix A.

$$\hat{c}_+ + \gamma \hat{c}_+ + \eta c_- \hat{d} = \sqrt{2\gamma} \hat{a}_+, \quad (2.9a)$$

$$\hat{c}_- + \gamma \hat{c}_- - \eta c_+ \hat{d}^{\dagger} = \sqrt{2\gamma} \hat{a}_-. \quad (2.9b)$$

The input-output relations are

$$\hat{b}_{\pm} = -\hat{a}_{\pm} + \sqrt{2\gamma} \hat{c}_{\pm} \quad (2.9c)$$

III. SOLUTION

Using the Hamiltonian formalism we obtain set of equations for the expectation values

$$\gamma C_+ + \eta C_- D = \sqrt{2\gamma} A_+, \quad (3.1a)$$

$$\gamma C_- - \eta^* C_+ D^* = \sqrt{2\gamma} A_-, \quad (3.1b)$$

$$\gamma_m D = \eta^* C_+ C_-^*, \quad (3.1c)$$

$$\gamma_m D^* = \eta C_+^* C_-. \quad (3.1d)$$

Introducing parameter $\nu = |\eta|^2 / \gamma \gamma_m$ we arrive at

$$C_+ \left(1 + \frac{\nu g^2 |A_-|^2}{(1 - \nu |C_+|^2)^2} \right) = \sqrt{\frac{2}{\gamma}} A_+, \quad (3.2a)$$

$$C_- \left(1 - \frac{\nu g^2 |A_+|^2}{(1 + \nu |C_-|^2)^2} \right) = \sqrt{\frac{2}{\gamma}} A_- \quad (3.2b)$$

The amplitudes C_+ , C_- are limited due to the ponderomotive nonlinearity. The classical resonant ponderomotive force creates mechanical oscillations with amplitude D which can be large. These oscillations are classical and can be suppressed using a regular force optimized for the known amplitudes of the probe fields. We also can use two orthogonal polarizations in the scheme shown in

Fig. 2 to reduce the undesirable resonant excitation of the mechanical oscillator (see Appendix B for details). In what follows we omit them from consideration and assume that $D = 0$ and $C_{\pm} = \sqrt{2/\gamma} A_{\pm}$.

A. Langevin equations

The equations of motion for the Fourier amplitudes of the operators describing the intracavity field as well as mechanical oscillator, c_{\pm} and d , can be written in form using (2.9a, 2.9b):

$$(\gamma - i\Omega)c_+(\Omega) + \eta C_- d(\Omega) = \sqrt{2\gamma}a_+(\Omega), \quad (3.3a)$$

$$(\gamma - i\Omega)c_-(\Omega) - \eta^* C_+ d^\dagger(-\Omega) = \sqrt{2\gamma}a_-(\Omega), \quad (3.3b)$$

$$(\gamma_m - i\Omega)d(\Omega) - \eta^* \left(C_-^* c_+(\Omega) + C_+ c_-^\dagger(-\Omega) \right) = \quad (3.3c)$$

$$= \sqrt{2\gamma_m}q(\Omega) + if_s(\Omega)$$

$$b_{\pm}(\Omega) = -a_{\pm}(\Omega) + \sqrt{2\gamma}c_{\pm}(\Omega), \quad (3.3d)$$

where b_{\pm} are the output Fourier amplitudes of the optical waves. The incident waves are in the coherent state, so the operators \hat{a}_{\pm} are characterized with the following commutators and correlators

$$[\hat{a}_{\pm}(t), \hat{a}_{\pm}^\dagger(t')] = \delta(t - t'), \quad (3.4)$$

$$\langle \hat{a}_{\pm}(t) \hat{a}_{\pm}^\dagger(t') \rangle = \delta(t - t'), \quad (3.5)$$

$\langle \dots \rangle$ stands for ensemble averaging.

The Fourier transform of these operators are introduced as follows

$$\hat{a}_{\pm}(t) = \int_{-\infty}^{\infty} a_{\pm}(\Omega) e^{-i\Omega t} \frac{d\Omega}{2\pi}. \quad (3.6)$$

Same is true for the other operators. Using (3.4) and (3.5) we derive commutators and correlators for the Fourier amplitudes of the input fluctuation operators

$$[a_{\pm}(\Omega), a_{\pm}^\dagger(\Omega')] = 2\pi \delta(\Omega - \Omega'), \quad (3.7)$$

$$\langle a_{\pm}(\Omega) a_{\pm}^\dagger(\Omega') \rangle = 2\pi \delta(\Omega - \Omega') \quad (3.8)$$

For the signal force we also introduce its Fourier amplitude assuming that the force is the resonant one acting during time interval τ :

$$F_S(t) = F_{s0} \cos(\omega_m t + \psi_f) = \quad (3.9)$$

$$= F_s(t) e^{-i\omega_m t} + F_s^*(t) e^{i\omega_m t}, \quad -\frac{\tau}{2} < t < \frac{\tau}{2},$$

$$f_s(\Omega) = \frac{F_s(\Omega)}{\sqrt{2\hbar\omega_m m}}, \quad f_{s0} = \frac{F_{s0}(\Omega)}{\sqrt{2\hbar\omega_m m}} = 2f_s. \quad (3.10)$$

where $F_s(\Omega)$ is the Fourier amplitude of the slow complex amplitude $F_s(t)$. In general case $F_s(\Omega) \neq F_s^*(-\Omega)$.

The thermal mechanical noise operators are described using expressions

$$[q(\Omega), q^\dagger(\Omega')] = 2\pi \delta(\Omega - \Omega'), \quad (3.11a)$$

$$\langle q(\Omega) q^\dagger(\Omega') \rangle = (2n_T + 1) 2\pi \delta(\Omega - \Omega'), \quad (3.11b)$$

$$n_T = \frac{\hbar\omega_m}{1 - e^{-\hbar\omega_m/\kappa_B T}}. \quad (3.11c)$$

Here κ_B is Boltzmann constant, T is the ambient temperature.

B. Solution of the Langevin equations

For the sake of simplicity we assume that the phases of the probe harmonics are selected so that

$$C_+ = C_+^* = C_- = C_-^* = C, \quad \eta = \eta^* \quad (3.12)$$

Introducing quadrature amplitudes

$$a_{\pm a} = \frac{a_{\pm}(\Omega) + a_{\pm}^\dagger(-\Omega)}{\sqrt{2}}, \quad (3.13a)$$

$$a_{\pm\phi} = \frac{a_{\pm}(\Omega) - a_{\pm}^\dagger(-\Omega)}{i\sqrt{2}}. \quad (3.13b)$$

and using (3.3) we obtain

$$(\gamma - i\Omega)c_{+a} + \eta C d_a = \sqrt{2\gamma}a_{+a}, \quad (3.14a)$$

$$(\gamma - i\Omega)c_{+\phi} + \eta C d_\phi = \sqrt{2\gamma}a_{+\phi}, \quad (3.14b)$$

$$(\gamma - i\Omega)c_{-a} - \eta C d_a = \sqrt{2\gamma}a_{-a}, \quad (3.14c)$$

$$(\gamma - i\Omega)c_{-\phi} + \eta C d_\phi = \sqrt{2\gamma}a_{-\phi}, \quad (3.14d)$$

$$(\gamma_m - i\Omega)d_a - \eta C (c_{+a} + c_{-a}) = \quad (3.14e)$$

$$= \sqrt{2\gamma_m}q_a - f_{s\phi}, \quad (3.14f)$$

$$(\gamma_m - i\Omega)d_\phi - \eta C (c_{+\phi} - c_{-\phi}) = \quad (3.14g)$$

$$= \sqrt{2\gamma_m}q_\phi + f_{sa}. \quad (3.14h)$$

Please note that sum $(c_{+a} + c_{-a})$ does not contain information on the mechanical motion (term $\sim d_a$ is absent), but produces the back action term in (3.14e).

Introducing

$$g_{a\pm} = \frac{c_{+a} \pm c_{-a}}{\sqrt{2}}, \quad g_{\phi\pm} = \frac{c_{+\phi} \pm c_{-\phi}}{\sqrt{2}}, \quad (3.15)$$

$$\alpha_{a\pm} = \frac{a_{+a} \pm a_{-a}}{\sqrt{2}}, \quad \alpha_{\phi\pm} = \frac{a_{+\phi} \pm a_{-\phi}}{\sqrt{2}}, \quad (3.16)$$

$$\beta_{a\pm} = \frac{b_{+a} \pm b_{-a}}{\sqrt{2}}, \quad \beta_{\phi\pm} = \frac{b_{+\phi} \pm b_{-\phi}}{\sqrt{2}} \quad (3.17)$$

and rewriting (3.14) in the new notations

$$(\gamma - i\Omega)g_{a+} = \sqrt{2\gamma}\alpha_{a+}, \quad (3.18a)$$

$$(\gamma - i\Omega)g_{a-} + \sqrt{2\eta}C d_a = \sqrt{2\gamma}\alpha_{a-}, \quad (3.18b)$$

$$(\gamma_m - i\Omega)d_a - \sqrt{2\eta}Cg_{a+} = \sqrt{2\gamma_m}q_a - f_{s\phi}, \quad (3.18c)$$

$$(\gamma - i\Omega)g_{\phi+} + \sqrt{2\eta}Cd_\phi = \sqrt{2\gamma}\alpha_{\phi+}, \quad (3.18d)$$

$$(\gamma - i\Omega)g_{-\phi} = \sqrt{2\gamma}\alpha_{\phi-}, \quad (3.18e)$$

$$(\gamma_m - i\Omega)d_\phi - \sqrt{2\eta}Cg_{\phi-} = \sqrt{2\gamma_m}q_\phi + f_{sa}. \quad (3.18f)$$

we find that sets (3.18a, 3.18b, 3.18c) and (3.18d, 3.18e, 3.18f) are decoupled.

It is convenient to present the solution of set (3.18a, 3.18b, 3.18c) for the amplitude quadratures in form

$$\beta_{+a} = \xi \alpha_{+a}, \quad \xi = \frac{\gamma + i\Omega}{\gamma - i\Omega}, \quad (3.19a)$$

$$\beta_{-a} = \xi \left(\alpha_{-a} - \frac{\mathcal{K} \alpha_{+a}}{\gamma_m - i\Omega} \right) - \quad (3.19b)$$

$$- \frac{\sqrt{\xi\mathcal{K}}}{\gamma_m - i\Omega} \left(\sqrt{2\gamma_m}q_a - f_{s\phi} \right), \quad (3.19c)$$

$$\mathcal{K} \equiv \frac{4\gamma\eta^2 C^2}{\gamma^2 + \Omega^2} \quad (3.19d)$$

As expected, in Eq. (3.19b) the back action term is proportional to the normalized probe power \mathcal{K} . However, this term can be excluded in the post processing. One can measure *both* β_{+a} and β_{-a} simultaneously and subtract β_{+a} from β_{-a} to remove the back action completely. It means that we can measure combination

$$\beta_{-a}^{\text{comb}} = \beta_{-a} + \xi \frac{\mathcal{K} \alpha_{+a}}{\gamma_m - i\Omega} = \quad (3.20)$$

$$= \xi \alpha_{-a} - \frac{\sqrt{\xi\mathcal{K}}}{\gamma_m - i\Omega} \left(\sqrt{2\gamma_m}q_a - f_{s\phi} \right), \quad (3.21)$$

which is completely back action free (!). This is the main finding of the study.

Let us write the force detection condition in terms of single-sided power spectral density $S_f(\Omega)$ recalculated to signal force (3.9). Demanding signal-to-noise ratio to exceed unity we get

$$f_{s0} \geq \sqrt{S_f(\Omega) \cdot \frac{\Delta\Omega}{2\pi}}, \quad (3.22)$$

where $\Delta\Omega \simeq 2\pi/\tau$. Using (3.8, 3.11b) we obtain for the case when we measure β_{-a} (3.19b)

$$S_f(\Omega) = 2\gamma_m(2n_T + 1) + \frac{(\gamma_m^2 + \Omega^2)}{|\mathcal{K}|} + |\mathcal{K}| \geq \quad (3.23)$$

$$\geq 2\gamma_m(2n_T + 1) + S_{SQL,f}, \quad (3.24)$$

$$S_{SQL,f} = 2\sqrt{\gamma_m^2 + \Omega^2} \quad (3.25)$$

The sensitivity is restricted by SQL. If we measure β_{-a}^{comb} (3.21) the spectral density is not limited by SQL

$$S_f(\Omega) = 2\gamma_m(2n_T + 1) + \frac{(\gamma_m^2 + \Omega^2)}{|\mathcal{K}|} \quad (3.26)$$

Here the first term describes thermal noise and the last one stands for the quantum measurement noise (shot

noise). The quantum measurement noise decreases with the power increase. The back action term is absent.

It worth noting that the thermal noise term is present in any opto-mechanical detection scheme. It can exceed the measurement error related to the measurement apparatus rather significantly. However, a proper measurement procedure allows to suppress this noise and also exclude the initial quantum uncertainty associated with the mechanical system. The main requirement for such a measurement is fast interrogation time, which should be much shorter than the ring down time of the mechanical system. This is possible if the measurement bandwidth exceeds the bandwidth of the mechanical mode. Sensitivity of narrowband resonant measurements is usually limited by the thermal noise.

Instead of the amplitude quadratures one can measure sum and differences of the phase quadratures. Solving set (3.18d, 3.18e, 3.18f) we arrive at

$$\beta_{-\phi} = \xi \alpha_{-\phi}, \quad (3.27a)$$

$$\beta_{+\phi} = \xi \left(\alpha_{+\phi} - \frac{\mathcal{K} \alpha_{-\phi}}{\gamma_m - i\Omega} \right) - \quad (3.27b)$$

$$- \frac{\sqrt{\xi\mathcal{K}}}{\gamma_m - i\Omega} \left(\sqrt{2\gamma_m}q_\phi + f_{sa} \right). \quad (3.27c)$$

We can measure quadratures $\beta_{\pm\phi}$ simultaneously and subtract back action proportional to $\beta_{-\phi}$ from $\beta_{+\phi}$.

Finally, a generalization is possible for a pair of quadratures with arbitrary parameter φ

$$b_{+\varphi} = b_{+a} \cos \varphi + b_{+\phi} \sin \varphi, \quad (3.28a)$$

$$b_{-\varphi} = b_{-a} \cos \varphi - b_{-\phi} \sin \varphi \quad (3.28b)$$

The sum $b_{+\varphi} + b_{-\varphi}$ is not disturbed by the mechanical motion but contains the term proportional to the back action force, whereas the difference $b_{+\varphi} - b_{-\varphi}$ contains the term proportional to mechanical motion (with back action and signal). The back action term can be measured and subtracted from the force measurement result.

IV. PARASITIC BACK ACTION

Fluctuation force acting on the mechanical oscillator is proportional to cross product ($c_- c_+^\dagger + c_-^\dagger c_+$) of the probe modes. In means that the fluctuation fields characterized with Fourier amplitude $\tilde{c}_-(\Omega) = c_-(\omega_- + 2\omega_m + \Omega)$ centered at frequencies in the vicinity of $\omega_- + 2\omega_m$ and Fourier amplitude $\tilde{c}_+(\Omega) = c_+(\omega_+ - 2\omega_m + \Omega)$ centered at frequency in the vicinity of $\omega_+ - 2\omega_m$ (see Fig. 3) contribute to the ponderomotive fluctuation force impinged by the light on the mirror. We marked with a tilde these complex amplitudes of the input and output waves for the sake of shortness. We neglected by these harmonic in the analysis above because the amplitude of the harmonics can be small. In what follow we take them into account and find the limitations they introduce for the proposed here measurement strategy.

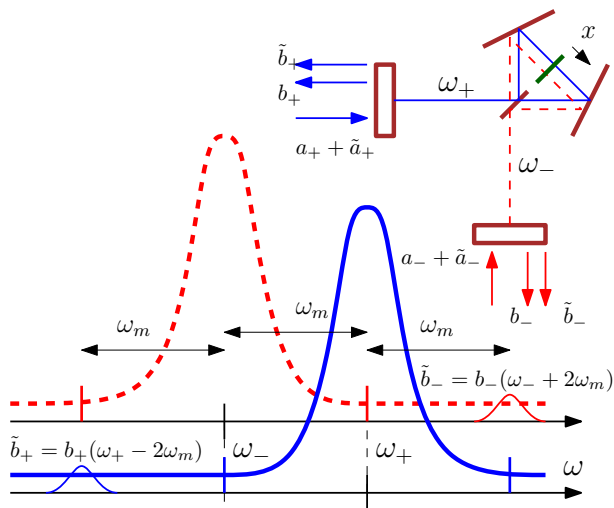


Figure 3: Side bands $\tilde{c}_{\pm} = c_{\pm}(\omega_{\pm} \mp 2\omega_m)$ inside cavity produce parasitic back action force acting on mechanical oscillator. We assume that one can measure waves b_{\pm} and side bands \tilde{b}_{\pm} separately.

Parasitic side bands provide additional terms to the expressions of the optical fields, for instance, (3.21) should be rewritten as

$$\beta_{-a}^{\text{comb}} = \xi \left(\alpha_{-a} + \frac{\mathcal{K}\tilde{g}_{a+}}{(\gamma_m - i\Omega)} \cdot \frac{(\gamma - i\Omega)}{\sqrt{2\gamma}} - \frac{\sqrt{\xi}\mathcal{K}}{\gamma_m - i\Omega} \left(\sqrt{2\gamma_m}q_a - f_s\phi \right) \right), \quad (4.1)$$

where noise term \tilde{g}_{a+} , defined by (C9), at condition (2.2) is approximately equal to

$$\tilde{g}_{a+} \simeq \frac{\sqrt{\gamma}}{2\omega_m} [\tilde{a}_{\phi+} - \tilde{a}_{\phi-}] \quad (4.2)$$

See details in Appendix C for details.

The back action created by the parasitic side bands limits sensitivity of the measurements. Instead of (3.23) we obtain a corrected expression for the single-sided power spectral density that can be presented as

$$S_f(\Omega) = 2\gamma_m(2n_T + 1) + \frac{(\gamma_m^2 + \Omega^2)}{|\mathcal{K}|} + \frac{|\mathcal{K}|(\gamma^2 + \Omega^2)}{4\omega_m^2} \geq \geq 2\gamma_m(2n_T + 1) + \frac{\sqrt{\gamma^2 + \Omega^2}}{2\omega_m} \cdot S_{SQL,f} \quad (4.3)$$

While the sensitivity still can be less than SQL at conditions (2.2), the sensitivity becomes limited after the probe power reaches the optimal value found from Eq. (4.3)

$$|\mathcal{K}|^2 = 4\omega_m^2 \frac{\gamma_m^2 + \Omega^2}{\gamma^2 + \Omega^2} \gg |\mathcal{K}_{SQL}|^2, \quad (4.4)$$

where \mathcal{K}_{SQL} corresponds the optimal power value needed to reach SQL in the system.

The impact of the parasitic harmonics can be reduced if one is able to measure $\tilde{b}_-(\Omega) = b_-(\omega_- + 2\omega_m + \Omega)$ as well as $\tilde{b}_+(\Omega) = b_+(\omega_- - 2\omega_m + \Omega)$ independently on the other spectral components of the output light. The measurement can be performed if narrow band pass filters are available.

The scheme of such a measurement is illustrated by Fig. 3. Measurement of optimally selected quadratures of b_{\pm} allows partial reduction of the parasitic back action described by term $\sim \tilde{g}_{a+}$ in (4.1). The reduction factor is $R \simeq \Omega/2\omega_m \ll 1$ (see details in Appendix D).

It means that in case $\gamma_m = 0$ and at conditions (2.2) the formula (4.3) will have form

$$S_f(\Omega) = \frac{\Omega^2}{|\mathcal{K}|} + \frac{|\mathcal{K}|\gamma^2\Omega^2}{16\omega_m^4} \geq \frac{\gamma|\Omega|}{2\omega_m^2} \cdot S_{SQL,f} \quad (4.5)$$

The sensitivity (4.5) is better than one defined by (4.3) achieved for the case of not suppressed parasitic harmonics.

V. DISCUSSION AND CONCLUSION

In the transducers shown in the schemes Fig. 1 and Fig. 2 the information on the mechanical *quadratures* transfers to the optical quadratures. The measurement of the difference of the optical amplitude quadratures is equivalent to the registration of the mechanical amplitude quadrature, whereas the measurement of the sum of the optical phase quadratures corresponds to the registration of mechanical phase quadrature, as shown by Eq. (3.14). This is a peculiar property of the parametric interaction.

One of the main features of the proposed here measurement strategy is in the usage of the dichromatic probe field results in the two independent quantum outputs. It gives us a flexibility to measure back action separately and then subtract it completely from the measurement result. The subtraction can be made in a broad frequency band.

In contrast, in conventional variational measurements [25–27] there is only one quantum output and the back action cannot be measured separately from the signal. Measurement of the linear combination of the amplitude and phase quadratures in that case allows partial subtraction of the back action. Only one quadrature of the output wave has to be measured to surpass SQL.

The scheme proposed here allows measurement either of a combination of sum and difference amplitude quadratures (3.21) or sum and difference of phase quadratures (3.27). Generalization (3.28) is also possible. These measurement lead to back action evasion in a broad frequency band. We expect that this technique will find a realization in other metrological configurations.

We propose to use filtration of output waves in order to depress back action due to parasitic side bands. Experimental realization of this filtration is not a simple task, but it is possible *in principle*.

Acknowledgments

The research of SPV and AIN has been supported by the Russian Foundation for Basic Research (Grant No. 19-29-11003), the Interdisciplinary Scientific and Educational School of Moscow University “Fundamental and Applied Space Research” and from the TAPIR GIFT MSU Support of the California Institute of Technology. The reported here research performed by ABM was carried out at the Jet Propulsion Laboratory, California Institute of Technology, under a contract with the National Aeronautics and Space Administration (80NM0018D0004). This document has LIGO number ???.

Appendix A: Derivation of the intracavity fields

Here we provide details of calculation for intracavity fields, for example, see [44].

We begin with Hamiltonian (2.4)

$$H = H_0 + H_{\text{int}} + H_T + H_\gamma + H_{T,m} + H_{\gamma_m}, \quad (\text{A1})$$

$$H_T = \sum_{k=0}^{\infty} \hbar \omega_k b_k^\dagger b_k, \quad (\text{A2})$$

$$H_\gamma = i\hbar \sqrt{\frac{\gamma \Delta \omega}{\pi}} \sum_{k=0}^{\infty} \left[(c_+^\dagger + c_-^\dagger) b_k - (c_+ + c_-) b_k^\dagger \right], \quad (\text{A3})$$

$$H_{T,m} = \sum_{k=0}^{\infty} \hbar \omega_k q_k^\dagger q_k, \quad (\text{A4})$$

$$H_{\gamma_m} = i\hbar \sqrt{\frac{\gamma \Delta \omega}{\pi}} \sum_{k=0}^{\infty} \left[d^\dagger q_k - dq_k^\dagger \right]. \quad (\text{A5})$$

Here H_T is the Hamiltonian of the environment presented as a bath of oscillators described with frequencies $\omega_k = \omega_{k-1} + \Delta\omega$ and annihilation and creation operators b_k, b_k^\dagger . H_γ is the Hamiltonian of coupling between the environment and the optical resonator, γ is the coupling constant. Similarly $H_{T,m}$ is the Hamiltonian of the environment presented by a thermal bath of mechanical oscillators with frequencies $\omega_k = \omega_{k-1} + \Delta\omega$ and amplitudes described with annihilation and creation operators q_k, q_k^\dagger . H_{γ_m} is the Hamiltonian of coupling between the environment and the mechanical oscillator, $2\gamma_m$ is the decay rate of the oscillator.

We write Heisenberg equations for operators c_+ and b_k :

$$i\hbar \dot{c}_+ = [c_+, H] = \hbar \omega_+ c_+ - i\hbar \eta c_- d + i\hbar \sqrt{\frac{\gamma \Delta \omega}{\pi}} \sum_{k=0}^{\infty} b_k, \quad (\text{A6a})$$

$$i\hbar \dot{b}_k = [b_k, H] = \hbar \omega_k b_k - i\hbar \sqrt{\frac{\gamma \Delta \omega}{\pi}} (c_+ + c_-) \quad (\text{A6b})$$

We introduce slow amplitudes $c_\pm \rightarrow c_\pm e^{-i\omega_\pm t}$, $d \rightarrow d e^{-i(\omega_+ - \omega_-)t}$, $b_k \rightarrow b_k e^{-i\omega_k t}$ and substitute them into (A6)

$$\dot{c}_+ = -\eta c_- d + \sqrt{\frac{\gamma \Delta \omega}{\pi}} \sum_{k=0}^{\infty} b_k e^{-i(\omega_k - \omega_+)t}, \quad (\text{A7a})$$

$$\dot{b}_k = -\sqrt{\frac{\gamma \Delta \omega}{\pi}} \left(c_+ e^{-i(\omega_+ - \omega_k)t} + c_- e^{-i(\omega_- - \omega_k)t} \right) \quad (\text{A7b})$$

Using initial condition $b_k(t=0) = b_k(0)$ to integrate (A7b) we obtain

$$b_k(t) = b_k(0) - \int_0^t \sqrt{\frac{\gamma \Delta \omega}{\pi}} c_+(s) e^{-i(\omega_+ - \omega_k)s} ds - \quad (\text{A8})$$

$$- \int_0^t \sqrt{\frac{\gamma \Delta \omega}{\pi}} c_-(s) e^{-i(\omega_- - \omega_k)s} ds \quad (\text{A9})$$

Using final condition $b_k(t=\infty) = b_k(\infty)$ to integrate (A7b) we derive

$$b_k(t) = b_k(\infty) + \int_t^\infty \sqrt{\frac{\gamma \Delta \omega}{\pi}} c_+(s) e^{-i(\omega_+ - \omega_k)s} ds - \quad (\text{A10})$$

$$+ \int_t^\infty \sqrt{\frac{\gamma \Delta \omega}{\pi}} c_-(s) e^{-i(\omega_- - \omega_k)s} ds \quad (\text{A11})$$

To get the input-output relation we substitute initial condition (A9) into (A7a)

$$\dot{c}_+ = -\eta c_- d + \sum_{k=0}^{\infty} \sqrt{\frac{\gamma \Delta \omega}{\pi}} b_k(0) e^{-i(\omega_k - \omega_+)t} - \quad (\text{A12a})$$

$$- \sum_{k=0}^{\infty} \int_0^t \frac{\gamma \Delta \omega}{\pi} c_+(s) e^{-i(\omega_k - \omega_+)(t-s)} ds - \quad (\text{A12b})$$

$$- \left(\sum_{k=0}^{\infty} \int_0^t \frac{\gamma \Delta \omega}{\pi} c_-(s) e^{-i(\omega_k - \omega_-)(t-s)} ds \right) e^{i(\omega_+ - \omega_-)t}$$

and omit the last term proportional to $e^{i(\omega_+ - \omega_-)t}$ as fast oscillating, and define the input field

$$a_+(t) = \sum_{k=0}^{\infty} \sqrt{\frac{\Delta \omega}{2\pi}} b_k(0) e^{-i(\omega_k - \omega_+)t} \quad (\text{A13})$$

To calculate the remaining sum in (A12) we assume the limit $\Delta\omega \rightarrow 0$ and replace the sum by the integral using rule

$$\Delta\omega \sum_{k=0}^{\infty} \rightarrow \int_0^\infty d\omega_k \quad (\text{A14a})$$

$$\begin{aligned}
& \sum_{k=0}^{\infty} \int_0^t \frac{\gamma \Delta \omega}{\pi} c_+(s) e^{-i(\omega_k - \omega_+)(t-s)} ds \rightarrow \quad (\text{A14b}) \\
& \rightarrow \int_0^{\infty} \int_0^t 2\gamma c_+(s) e^{-i(\omega_k - \omega_+)(t-s)} ds \frac{d\omega_k}{2\pi} = \\
& = \int_{-\omega_+}^{\infty} \int_0^t 2\gamma c_+(s) e^{-i\omega(t-s)} ds \frac{d\omega}{2\pi} \approx \\
& \approx \int_{-\infty}^{\infty} \int_0^t 2\gamma c_+(s) e^{-i\omega(t-s)} ds \frac{d\omega}{2\pi} = \\
& = \int_0^t 2\gamma c_+(s) \delta(t-s) ds = \frac{2\gamma c_+(t)}{2} = \gamma c_+(t) \quad (\text{A14c})
\end{aligned}$$

Substituting (A13) and (A14) into (A12) we obtain

$$\dot{c}_+ = -\eta c_- d + \sqrt{2\gamma} a_+ - \gamma c_+ \quad (\text{A15})$$

$$\dot{c}_+ + \gamma c_+ + \eta c_- d = \sqrt{2\gamma} a_+. \quad (\text{A16})$$

By analogue we derive the equation for input field a_- and present it in the similar form

$$a_-(t) = \sum_{k=0}^{\infty} \sqrt{\frac{\Delta \omega}{2\pi}} b_k(0) e^{-i(\omega_k - \omega_-)t} \quad (\text{A17})$$

It leads to the equation for the intracavity field c_-

$$\dot{c}_- + \gamma c_- - \eta c_+ d^\dagger = \sqrt{2\gamma} a_-. \quad (\text{A18})$$

Similar equation can be derived for the amplitude $q(t)$ of the mechanical oscillator

$$q(t) = \sum_{k=0}^{\infty} \sqrt{\frac{\Delta \omega}{2\pi}} b_{m,k}(0) e^{-i(\omega_k - \omega_+)t} \quad (\text{A19})$$

and get Langevine equation for mechanical oscillator's quadrature d

$$\dot{d} + \gamma_m d - \eta^* c_+ c_-^\dagger = \sqrt{2\gamma_m} q. \quad (\text{A20})$$

To get the output relation we substitute (A11) into (A7a) and define the output fields

$$b_+(t) = - \sum_{k=0}^{\infty} \sqrt{\frac{\Delta \omega}{2\pi}} b_k(\infty) e^{-i(\omega_k - \omega_+)t} \quad (\text{A21})$$

$$b_-(t) = - \sum_{k=0}^{\infty} \sqrt{\frac{\Delta \omega}{2\pi}} b_k(\infty) e^{-i(\omega_k - \omega_+)t}. \quad (\text{A22})$$

It leads to

$$\dot{c}_+ - \gamma c_+ + \eta c_- d = \sqrt{2\gamma} b_+ \quad (\text{A23})$$

$$\dot{c}_- - \gamma c_- + \eta^* c_+ d^\dagger = \sqrt{2\gamma} b_- \quad (\text{A24})$$

Utilizing pairs of equations (A16) and (A23) as well as (A18) and (A24) we obtain the final expression for the input-output relations

$$b_+ = -a_+ + \sqrt{2\gamma} c_+ \quad (\text{A25})$$

$$b_- = -a_- + \sqrt{2\gamma} c_- \quad (\text{A26})$$

Let us to derive the commutation relations for the Fourier amplitudes of the operators. We introduce Fourier transform of field $a_+(t)$ using (A13)

$$a_+(\Omega) = \int_{-\infty}^{\infty} \sum_{k=0}^{\infty} \sqrt{\frac{\Delta \omega}{2\pi}} b_k(0) e^{-i(\omega_k - \omega_+ - \Omega)t} dt = \quad (\text{A27a})$$

$$= \sum_{k=0}^{\infty} \sqrt{2\pi \Delta \omega} b_k(0) \delta(\Omega - \omega_k + \omega_+) \quad (\text{A27b})$$

This allows us to find the commutators (3.7):

$$\begin{aligned}
[a_+(\Omega), a_+^\dagger(\Omega')] &= \sum_{k=0}^{\infty} 2\pi \Delta \omega [b_k(0), b_k^\dagger(0)] \times \\
&\times \delta(\Omega - \omega_k + \omega_+) \delta(\Omega' - \omega_k + \omega_+) \rightarrow \\
&\rightarrow \int_{-\infty}^{\infty} 2\pi [b(0), b^\dagger(0)] \delta(\Omega - \omega) \delta(\Omega' - \omega) d\omega = \\
&= 2\pi \delta(\Omega - \Omega'), \quad (\text{A28a})
\end{aligned}$$

and the correlators (3.8)

$$\begin{aligned}
\langle a_+(\Omega), a_+^\dagger(\Omega') \rangle &= \sum_{k=0}^{\infty} 2\pi \Delta \omega \langle b_k(0), b_k^\dagger(0) \rangle \times \\
&\times \delta(\Omega - \omega_k + \omega_+) \delta(\Omega' - \omega_k + \omega_+) \rightarrow \\
&\rightarrow \int_{-\infty}^{\infty} 2\pi \langle b(0), b^\dagger(0) \rangle \delta(\Omega - \omega) \delta(\Omega' - \omega) d\omega = \\
&= 2\pi \delta(\Omega - \Omega') \quad (\text{A29a})
\end{aligned}$$

Similar expressions can be derived for commutators and correlators of the optical a_- and mechanical q quantum amplitudes.

Appendix B: Suppression of the resonant ponderomotive excitation

In this section we discuss possibilities of suppression of resonant ponderomotive excitation of the mechanical oscillations of the system.

We assume that there exist modes c_+ , e_+ characterized with orthogonal polarizations and the same geometrical path. These modes are characterized with eigen frequency ω_+ . Similarly, modes c_- , e_- are characterized with orthogonal polarizations and the same eigen frequency ω_- . In this configuration (2.4):

$$H = \tilde{H}_0 + \tilde{H}_{\text{int}} + H_\gamma, \quad (\text{B1a})$$

$$\tilde{H}_0 = \hbar\omega_+ c_+^\dagger c_+ + \hbar\omega_- c_-^\dagger c_- \quad (\text{B1b})$$

$$+ \hbar\omega_+ e_+^\dagger e_+ + \hbar\omega_- e_-^\dagger e_- + \hbar\omega_m d^\dagger d, \quad (\text{B1c})$$

$$\tilde{H}_{\text{int}} = \frac{\hbar}{i} \left(\eta c_+^\dagger c_- d - \eta^* c_+ c_-^\dagger d^\dagger \right) + \quad (\text{B1d})$$

$$+ \frac{\hbar}{i} \left(\eta_e e_+^\dagger e_- d - \eta_e^* e_+ e_-^\dagger d^\dagger \right) \quad (\text{B1e})$$

For the mean amplitude D we derive

$$\gamma_m D = \eta^* C_+ C_-^* + \eta_e E_+ E_-^* \quad (\text{B2})$$

Optimizing pumps of additional modes in a proper way one can make right part in (B2) to be zero.

The technique of suppression of the resonant ponderomotive excitation of the mechanical oscillations should not introduce undesirable fluctuations that cannot be removed by the measurement procedure. There at least two possibilities:

- Coupling constants are equal $\eta = \eta_e$ for both parts (B1d) and (B1e) of \tilde{H}_{int} . The additional back action originated from modes e_\pm can be evaded if we measure outputs of the four modes simultaneously.
- Coupling constant η_e is small ($\eta_e \ll \eta$). It can be realized by engineering coating of mirror M on Fig. 2. The larger pumps E_\pm can compensate regular force in (B2), without introducing significant back action noise.

Appendix C: Account of parasitic side bands

In this section we provide details of calculations taking into account the parasitic optical harmonics in the system.

We keep in mind that fluctuation fields in “+” and “-” cavities are not correlated with each other. Let us generalize interaction Hamiltonian (2.4c), assuming coupling constant η to be real:

$$\tilde{H}_{\text{int}} \simeq \frac{\hbar\eta}{i} \left\{ \left[C_+^* c_- + C_- c_+^\dagger \right] d - \left[C_-^* c_+ + C_+ c_-^\dagger \right] d^\dagger + \right. \quad (\text{C1a})$$

$$\left. + \left[C_+^* \tilde{c}_- + C_- \tilde{c}_+^\dagger \right] d^\dagger - \left[C_+ \tilde{c}_-^\dagger + C_-^* \tilde{c}_+ \right] d \right\} \quad (\text{C1b})$$

Here terms (C1a) correspond to conventional optomechanical coupling including back action, whereas terms (C1b) corresponds to parasitic back action due to the high frequency side bands \tilde{c}_\pm .

The additional terms appear in the set of Hamilton equations (3.3c) for the mechanical operators

$$(\gamma_m - i\Omega)d(\Omega) = \eta \left[C_+ c_-^\dagger(-\Omega) + C_-^* c_+(\Omega) \right] - \quad (\text{C2a})$$

$$- \eta \left[C_+^* \tilde{c}_-(\Omega) - C_- \tilde{c}_+^\dagger(-\Omega) \right] + \quad (\text{C2b})$$

$$+ \sqrt{2\gamma_m} q(\Omega) + i f_s(\Omega), \quad (\text{C2c})$$

where terms (C2b) describe the contributions due to the parasitic back action due to (C1b).

The operators c_\pm obey (3.3). For the operators of the parasitic sidebands inside the cavity we derive

$$\tilde{c}_+(\Omega)(\gamma + 2i\omega_m - i\Omega) = \sqrt{2\gamma} \tilde{a}_+(\Omega) - \quad (\text{C3a})$$

$$- \eta C_- d^\dagger(-\Omega), \quad \tilde{a}_+(\Omega) = a_+(-2\omega_m + \Omega), \quad (\text{C3b})$$

$$\tilde{c}_-(\Omega)(\gamma - 2i\omega_m - i\Omega) = \sqrt{2\gamma} \tilde{a}_-(\Omega) + \quad (\text{C3c})$$

$$+ \eta C_+ d(\Omega), \quad \tilde{a}_-(\Omega) = a_-(2\omega_m + \Omega). \quad (\text{C3d})$$

For *output* amplitudes of parasitic sidebands we find

$$\tilde{b}_+(\Omega) = \frac{\gamma - 2i\omega_m + i\Omega}{\gamma + 2i\omega_m - i\Omega} \tilde{a}_+(\Omega) - \frac{\sqrt{2\gamma} \eta C_- d^\dagger(-\Omega)}{\gamma + 2i\omega_m - i\Omega}, \quad (\text{C4a})$$

$$\tilde{b}_-(\Omega) = \frac{\gamma + 2i\omega_m + i\Omega}{\gamma - 2i\omega_m - i\Omega} \tilde{a}_-(\Omega) + \frac{\sqrt{2\gamma} \eta C_+ d(\Omega)}{\gamma - 2i\omega_m - i\Omega}, \quad (\text{C4b})$$

1. Quadratures

Let us consider the case of resonance probe light (3.12), find quadratures for parasitic optical harmonics and rewrite the expression (C2) for the mechanical quadratures as

$$\tilde{c}_{a\pm} = \frac{\tilde{c}_\pm(\Omega) + \tilde{c}_\pm^\dagger(-\Omega)}{\sqrt{2}}, \quad \tilde{c}_{\phi\pm} = \frac{\tilde{c}_\pm(\Omega) - \tilde{c}_\pm^\dagger(-\Omega)}{i\sqrt{2}} \quad (\text{C5a})$$

$$(\gamma_m - i\Omega)d_a = \eta C [c_{a-} + c_{a+}] - \quad (\text{C5b})$$

$$- \eta C [\tilde{c}_{a-} - \tilde{c}_{a+}] + \sqrt{2\gamma_m} q_a - f_{\phi s}, \quad (\text{C5c})$$

$$(\gamma_m - i\Omega)d_\phi = \eta C [-c_{\phi-} + c_{\phi+}] - \quad (\text{C5d})$$

$$- \eta C [\tilde{c}_{\phi-} + \tilde{c}_{\phi+}] + \sqrt{2\gamma_m} q_\phi + f_{as} \quad (\text{C5e})$$

Substituting (C5) into (3.3a, 3.3b) we get

$$c_{a+} = \frac{\sqrt{2\gamma} a_{a+}}{\gamma - i\Omega} - \frac{\eta^2 C^2 [c_{a-} + c_{a+} - \tilde{c}_{a-} - \tilde{c}_{a+}]}{(\gamma_m - i\Omega)(\gamma - i\Omega)} - \quad (\text{C6a})$$

$$- \eta C \cdot \frac{\sqrt{2\gamma_m} q_a - f_{\phi s}}{(\gamma_m - i\Omega)(\gamma - i\Omega)} \quad (\text{C6a})$$

$$c_{a-} = \frac{\sqrt{2\gamma} a_{a-}}{\gamma - i\Omega} + \frac{\eta^2 C^2 [c_{a-} + c_{a+} - \tilde{c}_{a-} - \tilde{c}_{a+}]}{(\gamma_m - i\Omega)(\gamma - i\Omega)} - \quad (\text{C6b})$$

$$+ \eta C \cdot \frac{\sqrt{2\gamma_m} q_a - f_{\phi s}}{(\gamma_m - i\Omega)(\gamma - i\Omega)} \quad (\text{C6b})$$

$$c_{\phi+} = \frac{\sqrt{2\gamma} a_{\phi+}}{\gamma - i\Omega} - \frac{\eta^2 C^2 [-c_{\phi-} + c_{\phi+} - \tilde{c}_{\phi-} + \tilde{c}_{\phi+}]}{(\gamma_m - i\Omega)(\gamma - i\Omega)} - \quad (\text{C6c})$$

$$- \eta C \cdot \frac{\sqrt{2\gamma_m} q_\phi + f_{as}}{(\gamma_m - i\Omega)(\gamma - i\Omega)} \quad (\text{C6c})$$

$$c_{\phi-} = \frac{\sqrt{2\gamma} a_{\phi-}}{\gamma - i\Omega} - \frac{\eta^2 C^2 [-c_{\phi-} + c_{\phi+} - \tilde{c}_{\phi-} + \tilde{c}_{\phi+}]}{(\gamma_m - i\Omega)(\gamma - i\Omega)} - \quad (\text{C6d})$$

$$- \eta C \cdot \frac{\sqrt{2\gamma_m} q_\phi + f_{as}}{(\gamma_m - i\Omega)(\gamma - i\Omega)} \quad (\text{C6d})$$

We introduce sum and difference quadratures for the parasitic sidebands, similarly to (3.15, 3.16, 3.17):

$$\tilde{g}_{a\pm} = \frac{\tilde{c}_{+a} \pm \tilde{c}_{-a}}{\sqrt{2}}, \quad \tilde{g}_{\phi\pm} = \frac{\tilde{c}_{+\phi} \pm \tilde{c}_{-\phi}}{\sqrt{2}}, \quad (\text{C7a})$$

$$\tilde{\alpha}_{a\pm} = \frac{\tilde{a}_{+a} \pm \tilde{a}_{-a}}{\sqrt{2}}, \quad \tilde{\alpha}_{\phi\pm} = \frac{\tilde{a}_{+\phi} \pm \tilde{a}_{-\phi}}{\sqrt{2}}, \quad (\text{C7b})$$

$$\tilde{\beta}_{a\pm} = \frac{\tilde{b}_{+a} \pm \tilde{b}_{-a}}{\sqrt{2}}, \quad \tilde{\beta}_{\phi\pm} = \frac{\tilde{b}_{+\phi} \pm \tilde{b}_{-\phi}}{\sqrt{2}} \quad (\text{C7c})$$

and arrive to the expressions for the sum and difference quadratures

$$g_{a+} = \frac{\sqrt{2\gamma} \alpha_{a+}}{\gamma - i\Omega}, \quad (\text{C8a})$$

$$g_{a-} = \frac{\sqrt{2\gamma} \alpha_{a-}}{\gamma - i\Omega} - \frac{2\eta^2 C^2 [g_{a+} - \tilde{g}_{a+}]}{(\gamma_m - i\Omega)(\gamma - i\Omega)} \quad (\text{C8b})$$

$$- \sqrt{2} \eta C \cdot \frac{\sqrt{2\gamma_m} q_a - f_{\phi s}}{(\gamma_m - i\Omega)(\gamma - i\Omega)}, \quad (\text{C8c})$$

$$g_{\phi-} = \frac{\sqrt{2\gamma} \alpha_{\phi-}}{\gamma - i\Omega}, \quad (\text{C8d})$$

$$g_{\phi+} = \frac{\sqrt{2\gamma} \alpha_{\phi+}}{\gamma - i\Omega} - \frac{2\eta^2 C^2 [g_{\phi-} + \tilde{g}_{\phi-}]}{(\gamma_m - i\Omega)(\gamma - i\Omega)} \quad (\text{C8e})$$

$$- \sqrt{2} \eta C \cdot \frac{\sqrt{2\gamma_m} q_\phi + f_{as}}{(\gamma_m - i\Omega)(\gamma - i\Omega)}. \quad (\text{C8f})$$

At the next step we evaluate the sum and difference quadratures of side bands using (C3)

$$\tilde{g}_{a+} = \frac{\sqrt{2\gamma}}{2} \left(\frac{\tilde{a}_+(\Omega) + \tilde{a}_+^\dagger(-\Omega)}{(\gamma + 2i\omega_m - i\Omega)} + \frac{\tilde{a}_+^\dagger(-\Omega) + \tilde{a}_-(\Omega)}{(\gamma - 2i\omega_m - i\Omega)} \right), \quad (\text{C9a})$$

$$\tilde{g}_{\phi-} = \frac{\sqrt{2\gamma}}{i2} \left(\frac{\tilde{a}_+(\Omega) + \tilde{a}_-^\dagger(-\Omega)}{(\gamma + 2i\omega_m - i\Omega)} - \frac{\tilde{a}_+^\dagger(-\Omega) + \tilde{a}_-(\Omega)}{(\gamma - 2i\omega_m - i\Omega)} \right). \quad (\text{C9b})$$

The combinations above do not contain any information on displacement of the mechanical oscillator.

For output sum and difference quadratures we obtain taking advantage of the Eq. (3.3d)

$$\beta_{a-} = \frac{\gamma + i\Omega}{\gamma - i\Omega} \alpha_{a-} - \sqrt{2\gamma} \frac{2\eta^2 C^2 [g_{a+} - \tilde{g}_{a+}]}{(\gamma_m - i\Omega)(\gamma - i\Omega)} \quad (\text{C10a})$$

$$- 2\sqrt{\gamma} \eta C \cdot \frac{\sqrt{2\gamma_m} q_a - f_{\phi s}}{(\gamma_m - i\Omega)(\gamma - i\Omega)} \quad (\text{C10b})$$

$$\beta_{a+} = \frac{\gamma + i\Omega}{\gamma - i\Omega} \alpha_{a+}, \quad (\text{C10c})$$

$$\beta_{\phi+} = \frac{\gamma + i\Omega}{\gamma - i\Omega} \alpha_{\phi+} - \sqrt{2\gamma} \frac{2\eta^2 C^2 [g_{\phi-} + \tilde{g}_{\phi-}]}{(\gamma_m - i\Omega)(\gamma - i\Omega)} \quad (\text{C10d})$$

$$- 2\sqrt{\gamma} \eta C \cdot \frac{\sqrt{2\gamma_m} q_\phi + f_{as}}{(\gamma_m - i\Omega)(\gamma - i\Omega)}$$

$$g_{\phi-} = \frac{\gamma + i\Omega}{\gamma - i\Omega} \alpha_{\phi-}. \quad (\text{C10e})$$

Finally, we rewrite β_{a+} after compensation of the main back action term as (4.1).

We see that one can subtract completely the main ($\sim \alpha_{a+}$) term of the back action. The contribution of the parasitic harmonic ($\sim \tilde{g}_{a+}$) into back action limit the sensitivity of the measurement in this case. In the following section we discuss a possibility of reduction of their impact.

Appendix D: Reduction of the residual back action

Using (C9) we find

$$\tilde{\beta}_{a+} = \frac{1}{2} \left\{ \frac{\gamma - 2i\omega_m + i\Omega}{\gamma + 2i\omega_m - i\Omega} \cdot (\tilde{a}_+(\Omega) + \tilde{a}_+^\dagger(-\Omega)) \quad (\text{D1a}) \right.$$

$$\left. + \frac{\gamma + 2i\omega_m + i\Omega}{\gamma - 2i\omega_m - i\Omega} \cdot (\tilde{a}_+^\dagger(-\Omega) + \tilde{a}_-(\Omega)) \right\}, \quad (\text{D1b})$$

$$\tilde{\beta}_{\phi-} = \frac{1}{2i} \left\{ \frac{\gamma - 2i\omega_m + i\Omega}{\gamma + 2i\omega_m - i\Omega} (\tilde{a}_+(\Omega) + \tilde{a}_+^\dagger(-\Omega)) \quad (\text{D1c}) \right.$$

$$\left. - \frac{\gamma + 2i\omega_m - i\Omega}{\gamma - 2i\omega_m + i\Omega} \cdot (\tilde{a}_+^\dagger(-\Omega) + \tilde{a}_-(\Omega)) \right\}. \quad (\text{D1d})$$

In order to compensate ‘‘tilde’’ terms we have to measure a combination of arbitrary quadratures defined by phases φ_\pm

$$\tilde{b}_{\varphi+} = \frac{\tilde{b}_+(\Omega)e^{i\varphi+} + \tilde{b}_+^\dagger(\Omega)e^{-i\varphi+}}{\sqrt{2}}, \quad (\text{D2a})$$

$$\tilde{b}_{\varphi-} = \frac{\tilde{b}_-(\Omega)e^{i\varphi-} + \tilde{b}_-^\dagger(\Omega)e^{-i\varphi-}}{\sqrt{2}}. \quad (\text{D2b})$$

In order to remove parasitic terms we have to define the phases as follows

$$\varphi_+ = -\varphi_- = \varphi \quad \Rightarrow \quad (\text{D2c})$$

$$\frac{\tilde{b}_{\varphi+} + \tilde{b}_{\varphi-}}{\sqrt{2}} = \frac{\gamma - i2\omega_m + i\Omega}{2(\gamma + i2\omega_m - i\Omega)} (\tilde{a}_+(\Omega) + \tilde{a}_+^\dagger(-\Omega)) e^{i\varphi} \quad (\text{D2d})$$

$$+ \frac{\gamma + i2\omega_m + i\Omega}{2(\gamma - i2\omega_m - i\Omega)} (\tilde{a}_-(\Omega) + \tilde{a}_+^\dagger(-\Omega)) e^{-i\varphi}$$

We get for φ an approximate expression

$$(\gamma - i2\omega_m + i\Omega)e^{i\varphi} \simeq \text{const}, \quad (\text{D2d})$$

$$\Rightarrow e^{i\varphi} = \sqrt{\frac{\gamma + 2i\omega_m}{\gamma - 2i\omega_m}} \quad (\text{D2e})$$

Performing the same procedure we developed for the main harmonics of the probe light we find that the impact of the parasitic harmonics can be reduced by $R \simeq \Omega/2\omega_m$ (assuming validity of conditions (2.2)). After the compensation we obtain

$$\beta_{a-} = \frac{\xi\sqrt{\mathcal{K}}}{(\gamma_m - i\Omega)} \left\{ \frac{(\gamma_m - i\Omega)}{\sqrt{\mathcal{K}}} \alpha_{a-} - \sqrt{\mathcal{K}} \alpha_{a+} \right\} \quad (\text{D3})$$

$$+\sqrt{\mathcal{K}} \frac{(\gamma - i\Omega)}{\sqrt{2\gamma}} \tilde{g}_{a+} R - \sqrt{\xi^{-1}} \left[\sqrt{2\gamma_m} q_a - f_{\phi_s} \right] \Big\}.$$

instead of (4.1). The first term in braces $\sim \alpha_{a-}$ results from the quantum measurement noise and the second term $\sim \alpha_{a+}$ describes back action that can be removed

from the measurement results. The back action term due to the parasitic harmonics can be reduced. Optimization of contributions of these terms defines the ultimate sensitivity of the measurement technique that is better than the SQL.

-
- [1] LVC-Collaboration, “Prospects for Observing and Localizing Gravitational-Wave Transients with Advanced LIGO and Advanced Virgo,” *arXiv*, vol. 1304.0670, 2013.
- [2] J. Aasi *et al* (LIGO Scientific Collaboration) *et al.*, “Advanced LIGO,” *Classical and Quantum Gravity*, vol. 32, p. 074001, 2015.
- [3] D. Martynov *et al.*, “Sensitivity of the Advanced LIGO detectors at the beginning of gravitational wave astronomy,” *Physical Review D*, vol. 93, p. 112004, 2016.
- [4] F. Asernese *et al.*, “Advanced Virgo: a 2nd generation interferometric gravitational wave detector,” *Classical and Quantum Gravity*, vol. 32, p. 024001, 2015.
- [5] K. L. Dooley, J. R. Leong, T. Adams, C. Affeldt, A. Bisht, C. Bogan, J. Degallaix, C. Graf, S. Hild, and J. Hough, “GEO 600 and the GEO-HF upgrade program: successes and challenges,” *Classical and Quantum Gravity*, vol. 33, p. 075009, 2016.
- [6] Y. Aso, Y. Michimura, K. Somiya, M. Ando, O. Miyakawa, T. Sekiguchi, and D. Tats, “Interferometer design of the KAGRA gravitational wave detector,” *Physical Review D*, vol. 88, p. 043007, 2013.
- [7] S. Forstner and S. Prams and J. Knittel and E.D. van Ooijen and J.D. Swaim and G.I. Harris and A. Szorkovszky and W.P. Bowen and H. Rubinsztein-Dunlop, “Cavity Optomechanical Magnetometer,” *Physical Review Letters*, vol. 108, p. 120801, 2012.
- [8] B.-B. Li, J. Bielek, U. Hoff, L. Madsen, S. Forstner, V. Prakash, C. Schafermeier, T. Gehring, W. Bowen, and U. Andersen, “Quantum enhanced optomechanical magnetometry,” *Optica*, vol. 5, p. 850, 2018.
- [9] M. Wu, A.C. Hryciw, C. Healey, D.P. Lake, H. Jayakumar, M.R. Freeman, J.P. Davis, and P.E. Barclay, “Dissipative and dispersive optomechanics in a nanocavity torque sensor,” *Physical Review X*, vol. 4, p. 021052, 2014.
- [10] P. H. Kim, B. D. Hauer, C. Doolin, F. Souris, and J. P. Davis, “Approaching the standard quantum limit of mechanical torque sensing,” *Nature Communications*, vol. 7, p. 13165, 2016.
- [11] J. Ahn, Z. Xu, J. Bang, P. Ju, X. Gao, and T. Li, “Ultrasensitive torque detection with an optically levitated nanorotor,” *Nature Nanotechnology*, vol. 15, p. 89–93, 2020.
- [12] V.B. Braginsky, “Classic and quantum limits for detection of weak force on acting on macroscopic oscillator,” *Sov. Phys. JETP*, vol. 26, p. 831–834, 1968.
- [13] V.B. Braginsky and F.Ya. Khalili, *Quantum Measurement*. Cambridge University Press, Cambridge, 1992.
- [14] V.B. Braginsky and F.Ya. Khalili., “Gravitational wave antenna with QND speed meter,” *Physics Letters A*, vol. 147, p. 251–256, 1990.
- [15] V.B. Braginsky, M.L. Gorodetsky, F.Y. Khalili, and K.S. Thorne, “Dual-resonator speed meter for a free test mass,” *Physical Review D*, vol. 61, p. 044002, 2000.
- [16] V.B. Braginsky and F.Ya. Khalili, “Low noise rigidity in quantum measurements,” *Phys. Lett. A*, vol. 257, p. 241, 1999.
- [17] F.Ya. Khalili, “Frequency-dependent rigidity in large-scale interferometric gravitational-wave detectors,” *Physics Letters A*, vol. 288, p. 251–256, 2001.
- [18] The LIGO Scientific collaboration, “A gravitational wave observatory operating beyond the quantum shot-noise limit,” *Nature Physics*, vol. 73, p. 962–965, 2011.
- [19] LIGO Scientific Collaboration and Virgo Collaboration, “Enhanced sensitivity of the LIGO gravitational wave detector by using squeezed states of light,” *Nature Photonics*, vol. 7, p. 613–619, 2013.
- [20] V. Tse *et al.*, “Quantum-Enhanced Advanced LIGO Detectors in the Era of Gravitational-Wave Astronomy,” *Physical Review Letters*, vol. 123, p. 231107, 2019.
- [21] F. Asernese, *et al*, and (Virgo Collaboration), “Increasing the Astrophysical Reach of the Advanced Virgo Detector via the Application of Squeezed Vacuum States of Light,” *Physical Review Letters*, vol. 123, p. 231108, 2019.
- [22] M. Yap, J. Cripe, G. Mansell, *et al.*, “Broadband reduction of quantum radiation pressure noise via squeezed light injection,” *Nature Photonics*, vol. 14, p. 19–23, 2020.
- [23] H. Yu, L. McCuller, M. Tse, *et al.*, “Quantum correlations between light and the kilogram-mass mirrors of LIGO,” *Nature*, vol. 583, p. 43–27, 2020.
- [24] J. Cripe, N. Aggarwal, R. Lanza, *et al.*, “Measurement of quantum back action in the audio band at room temperature,” *Nature*, vol. 568, p. 364–367, 2019.
- [25] S.P. Vyatchanin and A.B. Matsko, “Quantum limit of force measurement,” *Sov.Phys - JETP*, vol. 77, p. 218–221, 1993.
- [26] S. Vyatchanin and E. Zubova, “Quantum variation measurement of force,” *Physics Letters A*, vol. 201, p. 269–274, 1995.
- [27] H.J. Kimble, Y. Levin, A.B. Matsko, K.S. Thorne, and S.P. Vyatchanin, “Conversion of conventional gravitational-wave interferometers into QND interferometers by modifying input and/or output optics,” *Phys. Rev. D*, vol. 65, p. 022002, 2001.
- [28] M. Tsang and C. Caves, “Coherent Quantum-Noise Cancellation for Optomechanical Sensors,” *Phys. Rev. Lett.*, vol. 105, p. 123601, 2010.
- [29] E. Polzik and K. Hammerer, “Trajectories without quantum uncertainties,” *Annalen de Physik*, vol. 527, p. A15–A20, 2014.
- [30] C. Moller, R. Thomas, G. Vasilakis, E. Zeuthen, Y. Tsaturyan, M. Balabas, K. Jensen, A. Schliesser, K. Hammerer, and E. Polzik, “Quantum back-action-evading measurement of motion in a negative mass reference frame,” *Nature*, vol. 547, p. 191–195, 2017.
- [31] A. B. Matsko, V. V. Kozlov, and M. O. Scully, “Back-

- action Cancellation in Quantum Nondemolition Measurement of Optical Solitons,” *Phys. Rev. Lett.*, vol. 82, p. 3244–3247, Apr 1999.
- [32] V. Braginsky, Y. Vorontsov, and K. Thorne, “Quantum Nondemolition Measurements,” *Science*, vol. 209, p. 547–557, 1980.
- [33] V. Braginsky, Yu.I.Vorontsov, and F. Y. Khalili *Sov. Phys. — JETP Lett.*, vol. 33, p. 405, 1981.
- [34] A. Clerk, F. Marquardt, and K. Jacobs, “Back-action evasion and squeezing of a mechanical resonator using a cavity detector,” *New Journal of Physics*, vol. 10, p. 095010, 2008.
- [35] E. Wollman, C. Lei, A. Weinstein, J. Suh, A. Kronwald, F. Marquardt, A. Clerk, and K. Schwab, “Quantum squeezing of motion in a mechanical resonator,” *Science*, vol. 349, no. 6251, p. 952–955, 2015.
- [36] J.-M. Pirkkalainen, E. Damskagg, M. Brandt, F. Massel, and M. Sillanpaa *Phys. Rev. Lett.*, vol. 115, p. 243601, 2015.
- [37] L. Buchmann, S. Schreppler, J. Kohler, N. Spethmann, and D. Stamper-Kurn, “Complex Squeezing and Force Measurement Beyond the Standard Quantum Limit,” *Physical Review Letters*, vol. 117, p. 030801, 2016.
- [38] S. Vyatchanin and A. Matsko, “On sensitivity limitations of a dichromatic optical detection of a classical mechanical force,” *Journal of Optical Society of America B*, vol. 35, p. 1970–1978, 2018.
- [39] M. L. Povinelli, M. Lončar, M. Ibanescu, E. J. Smythe, S. G. Johnson, F. Capasso, and J. D. Joannopoulos, “Evanescent-wave bonding between optical waveguides,” *Opt. Lett.*, vol. 30, p. 3042–3044, Nov 2005.
- [40] A. V. Maslov, V. N. Astratov, and M. I. Bakunov, “Resonant propulsion of a microparticle by a surface wave,” *Phys. Rev. A*, vol. 87, p. 053848, May 2013.
- [41] S.P. Vyatchanin and A.B. Matsko, “Quantum variation scheme of measurement of force and compensation of back action,” *Sov. Phys. – JETP*, vol. 82, p. 107, 1996.
- [42] A.B. Matsko and S.P. Vyatchanin, “A ponderomotive scheme for QND measurement of quadrature component,” *Applied Physics B*, vol. 64, no. 2, p. 167–171, 1997.
- [43] X. Li, M. Korobko, Y. Ma, R. Schnabel, and Y. Chen, “Coherent coupling completing an unambiguous optomechanical classification framework,” *Physical Review A*, vol. 100, p. 053855, 2019.
- [44] D. Walls and G. Milburn, *Quantum optics*. Springer-V Berlin Heidelberglag, 2008.